

# Performance Analysis of Restraint Grouting-Anchoring Lap Connection of Rebar in Prefabricated Shear Walls

Yuzhe SUN\*, Guoliang BAI

**Abstract:** This study aims to obtain the key engineering parameters for the reliability performance of restraint grouting-anchoring lap connection of rebar, so as to achieve the promotion of prefabricated building. To study the performance of restraint grouting-anchoring lap connection of rebar in prefabricated shear walls, four parameters rebar diameter, lap length, bellows diameter and concrete strength were selected as the main subjects of the test. Specimens were prepared according to four important parameters. The test results show that the connection performance is reliable in the specimen of restraint grouting-anchoring lap connection of rebar for pre-drilled bellows. Through theoretical analysis, a force model was proposed to provide a quantitative analysis method for the theoretical calculation of the mechanical properties of restraint grouting-anchoring lap connection of rebar. As the diameter of the rebar increases, the spread of concrete stresses in the specimens becomes more pronounced; as the diameter of the rebar increases, the spread of concrete stresses in the specimens becomes more pronounced; the shorter the lap length, the higher the bond stress between the rebar and the concrete interface in the specimen, the damage of the specimen is from mild to severe; as the strength of the concrete increases, a larger diameter of rebar and a shorter lap length are required to achieve the same damage pattern in the specimen.

**Keywords:** lap length; prefabricated building; restraint grouting-anchoring connection; theoretical calculation of the mechanical properties

## 1 INTRODUCTION

Prefabricated building is an effective way of housing industrialisation [1-4]. Prefabricated building technology is a new kind of building formed that building made of industrially produced components is assembled at the construction site through splicing. Traditional building products are mainly cast-in-place in a monotonous form. Compared with cast-in-place buildings, prefabricated buildings take some of the original cast-in-place components, such as shear walls, beams, columns and staircases, and produce them industrially in a factory. Prefabricated building has been widely studied and applied in the United States [5-7], Japan [8-11], Libya [12], China [13], Italy [14], Serbia [15], Australia [16, 17] and other countries. Prefabricated building is a practical means of achieving housing industrialisation, and the restraint grouting-anchoring connection method is the key to the construction of prefabricated buildings. The restraint grouting-anchoring connection that was studied in this paper will facilitate the development of Prefabricated building. This paper synthesizes the research on restraint grouting-anchoring connection in recent years, improves the traditional device and verifies the reliability.

Restraint grouting-anchoring connection has many years of research application outside China. The American Concrete Institute "Building Code Requirements for Structural Concrete" says that the transverse spacing between lapped bars in a flexural member must not be greater than the lesser of 1/5 of the lap length and 6". Sagan et al. [18] completed a text that provides data behaviour of noncontact lap splices subjected to repeated inelastic tensile loading, suggesting that non-contact lap splices can sustain somewhat more inelastic load cycles than contact lap splices and that a truss model is an accurate description of behaviour. Belleri and Riva [19] conducted experiments on the cyclic behaviour of column-to-foundation subassemblies of grouted sleeve connections. The grouted sleeves had a diameter of 70 mm. The length of embedded grouted sleeve was 1,150 mm. The results demonstrated that grouted sleeves ensure a ductility and energy dissipation capacity

similar to those of cast-in-place connections. Kulkarni et al. [20] presented a nonlinear finite element analysis of hybrid-steel concrete connections. The finite element models were validated using the experimental results of the hybrid-steel concrete connections. They also studied the critical parameters influencing the joint's behaviour. There are two main types of the restrained grouting anchorage connection technology that have been studied in China. The first one is the inserted pre-cast grouted reinforcement lap connection proposed by Harbin Institute of Technology, and the second one is the New Precast Concrete Structure grout-anchor connection introduced by Zhongnan Construction Group. Comparing the two modes, the former is equipped with spiral hoops in the reinforcement lap section, which can effectively restrain the diagonal extrusion cone wedge effect of the cross ribs between the lap bars, thus preventing the development of longitudinal splitting cracks, and the latter can effectively reduce the lap length of the bars.

This study aims to obtain the key engineering parameters for the reliability performance of restraint grouting-anchoring lap connection of rebar, so as to achieve the promotion of prefabricated building. To study the performance of restraint grouting-anchoring lap connection of rebar in prefabricated shear walls, four parameters rebar diameter, lap length, bellows diameter and concrete strength were selected as the main subjects of the test. Our team has completed the experimental design and testing of the performance of restraint grouting-anchoring lap connection of rebar in prefabricated shear walls. Theoretical analysis of some results was conducted. The insertion-type grouted rebar lap connection used in this paper is a rebar connection method for prefabricated concrete structures proposed by the Harbin Institute of Technology. The hole formation method is core pulling and the steel pipe with rib stiffener used for forming the hole needs to be pulled out after the concrete has set. This connection method has problems such as long prefabrication period, low production efficiency and tedious process. New prefabricated concrete (NPC) structural grouting-anchoring connection uses bellows to form holes. There is no lateral restraint and the hole formation method is simple. The performance design tests combined the

strengths of the two types of grouting-anchoring lap connections and optimised the grouting-anchoring lap connection method to form an inserted spiral hoop-bellows grouting-anchoring connection method and carried out experimental research. The performance of this connection was investigated in a one-way tensile test by selecting the main factors such as rebar diameter, hole size, lap length and concrete strength. The test results show that the connection performance is reliable in the specimen of restraint grouting-anchoring lap connection of rebar for pre-drilled bellows. Through theoretical analysis, a force model was proposed to provide a quantitative analysis method for the theoretical calculation of the mechanical properties of restraint grouting-anchoring lap connection of rebar.

## 2 OVERVIEW OF THE TEST

### 2.1 Wooden Formwork, Bellows, Rebar Processing

The size of the formwork, the length of the embedded rebar and inserted rebar, and the length of the metal bellows were determined according to the design parameters of the test, and reserved holes for rebar connection on the formwork. The bellows used for the test were required to comply with the current Chinese national industry standard "Metal Bellows for Prestressed Concrete" (JG 225-2007). The mild steel strip rolled in galvanized steel with inner diameter of 40 mm and 50 mm were used respectively. To ensure that the inserted rebar is located in the centre of the bellow, wooden rings of 40 mm and 50 mm in diameter were fabricated during the test preparation stage, with the inner diameter of the wooden rings being equal to the outer

diameter of the rebar, so that the rebar can pass through the wooden rings and enter the bellow. The wooden rings were 20 mm thick. The installation of wood rings grouted at both ends of the bellows is equivalent to the formation of a non-bonded area at both ends.

### 2.2 Spiral Hoop with Strain Gauges

To measure the strain changes in the spiral hoop during loading and to reflect the stress diffusion in the concrete of the specimen, two strain gauges were set respectively at 1/4 and 1/2 of the spiral hoop's steel surface in the direction of the loading end, and the outside of the installed strain gauges was protected with epoxy resin.

### 2.3 Embedded Rebars, Spiral Hoops and Metal Bellows Into the Mould

Components were assembled and positioned in accordance with the design drawings (Fig. 1). The installation sequence was as follows: the spiral hoop and metal bellows were first assembled into the mould; then the embedded rebar was inserted through the rebar holes at both ends of the formwork and ensured to penetrate inside the hoop; finally, the spiral hoop and embedded rebar were spot welded at the contact points to strengthen the connection. Hoop diameter is 6 mm, hoop ring diameter is 70 mm round spiral hoop, hoop spacing is 50 mm.

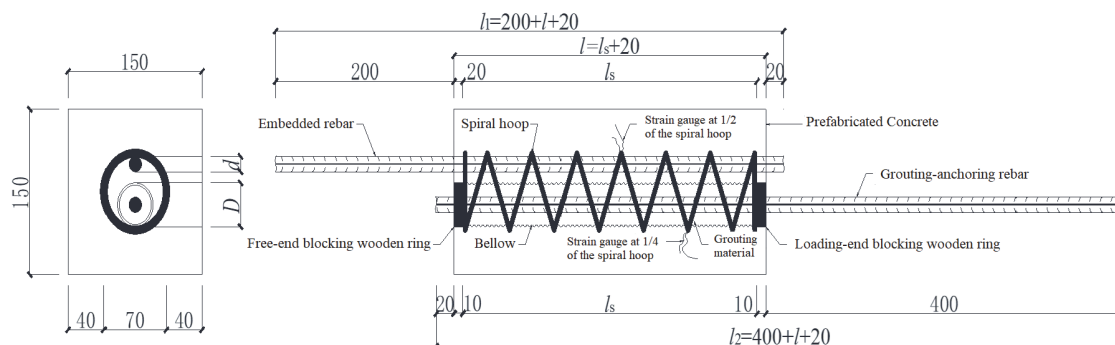


Figure 1 Specimen construction and dimensional drawings

### 2.4 Concrete Placement and Curing

Before the components were put into the mould, the inside of the formwork was required to be oiled to facilitate the demoulding operation of the specimen later; before concrete placement, the relative positions of the rebar, spiral hoop and bellows were rechecked; during the concrete placement process, attention should be paid to protecting the strain gauge leads and the strain gauge must not be touched during concrete vibrating. The specimens were demoulded after 7 days of curing in the standard condition. After 28 days of curing, the bellows can be grouted and inserted.

### 2.5 Grout and Insertion

In the test, a high-pressure grouting machine along with a blocking wooden ring was used to achieve semi-closed pressure grouting. The grouting material was completely

injected into the bellow and then inserted into the rebar. Internal vibrating and filling treatment were conducted to ensure that the grouting material completely wrapped the rebar and filled the entire bellow. The wooden ring can be used to seal both ends when the specimen is lying flat for maintenance, which prevents the grouting material from flowing out and ensures that the insertion of the rebar is accurately positioned.

### 2.6 Loading and Measurement of Specimen

The loading device was composed of a special steel frame and a 50 T piercing hydraulic jack. The special steel frame consisted of pressure-bearing steel plates, wire steel columns and bolts; the 50 T through-the-heart hydraulic jack consisted of a hydraulic jack, a hydraulic lever and a digital pressure gauge.

The test utilised different sizes of anchorages and hydraulic jacks to achieve a loading form with one end anchored and one end tensioned. Due to the non-contact lap of the rebar, the specimen was susceptible to eccentric bending moments during the loading process, so pads were placed around the specimen for moment balancing. The one-way tensile test was carried out according to the provisions of the Standard for Test Methods for Concrete Structures (GB 50152-2012). The loading method was uniform continuous loading at 5 kN/min, 6 kN/min and 12 kN/min respectively according to the size of the steel bar diameter until the specimen was damaged.

Displacement gauges were installed at the loading and free ends of the grouting-anchoring rebars to measure the corresponding displacements. Meanwhile, point records were made according to fixed time intervals; the JM3840 dynamic and static strain test system was used to measure the strain values of the spiral hoop bars; the load values were recorded by dedicated personnel at fixed time intervals by means of digital pressure gauges equipped with hydraulic jacks, and the time intervals corresponded to the point recording intervals of the displacement values, facilitating the mapping of the load-displacement curve at a later stage.

### 3 TEST RESULTS

#### 3.1 Test Phenomena

Two basic modes of damage occurred during loading of the specimens: rebar pull-out damage and bonded anchorage damage. Cracks of different forms and degrees appear on the surface of the specimen, and the specific cracking process is as follows.

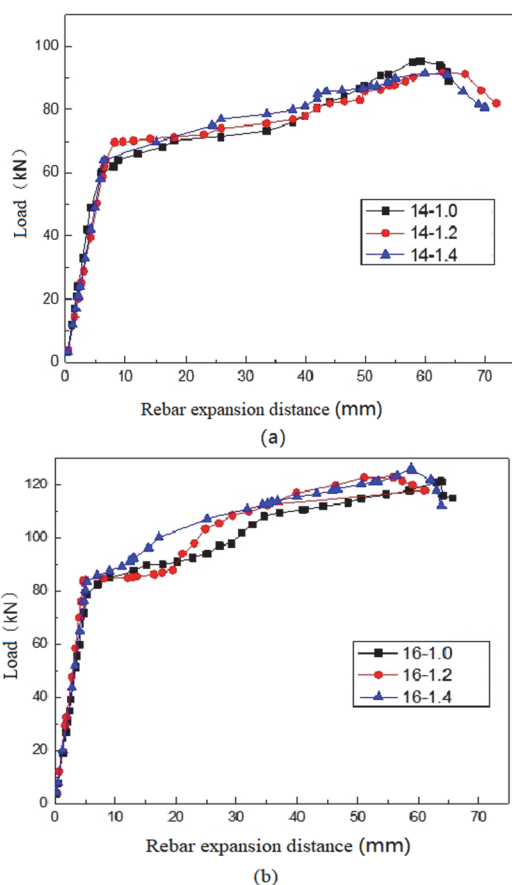


Figure 2 The rebar expansion distance-Load relationship (a) 3 samples of 14 mm rebar diameters, (b) 3 samples of 16 mm rebar diameters.

The rebar expansion distance-Load relationship are shown in Fig. 2. After the loading starts, the load elongation of the reinforcement increases linearly and proportionally, and the load reinforcement elongation curve is basically a straight line. After the stress of the reinforcement exceeds the elastic limit and enters the yield section, the load fluctuates but tends to stabilize overall. The curve appears a clear step. The specimen underwent rebar pull-out damage: as the load increased, the specimen developed initial cracks before the rebar yielded, concentrated in the middle of the specimen; the cracks appeared accompanied by a rattling sound. When the rebar entered the strengthened section, longitudinal splitting cracks appeared at both the anchoring and loading ends of the specimen. The cracks at the anchoring end appeared and continued to extend along the radial direction of the rebar to the surface of the specimen, and the concrete around the rebar fell off to different degrees during the loading process; the cracks at the loading end appeared and continued to extend in all directions along the bellow diameter. When the load was close to the ultimate value of the tensile strength of the rebar, transverse cracks began to appear one after another near the loading end of the specimen and interacted with the extended splitting cracks in a net-like manner. At the end of the loading period, a big sound came from the end of the specimen and eventually the rebar pulled off and broke.

The specimen underwent bonded anchorage damage: the specimen was initially loaded with no significant difference from other specimens; when loaded near the yield load of the rebar, longitudinal splitting cracks began to appear at both the loading and anchoring ends of the specimen. As the load continued to increase, the cracks developed rapidly and extended along the end face, with the crack width expanding rapidly. As the loading continued, the concrete at the end began to peel and fall off and the damage to the concrete block increased. Eventually, the specimen underwent anchorage damage. Significant slip values could be measured at the loading and free ends of the grouting-anchoring rebar, with no slip of the embedded rebar.

#### 3.2 Test Results

The data collected during the test loading were mainly load values, spiral hoop strain values and displacement meter values. The test data showed that the break yield ratio of the specimens was greater than 1 and that the grouting-anchoring rebars yielded in tension during loading. The lap length was not less than 0.7 times the basic anchorage length and the final damage was in the form of rebar pull-out for the 14 mm and 16 mm longitudinal specimens. This shows that grouting-anchoring lap connections are designed for reliable specimen performance and that the specimen yielding and damage are mainly influenced by the performance of the rebar when the lap length meets the requirements. The test specimen with a lap length of  $0.6 l_a$  was damaged by splitting of the concrete block and the damage load was similar to the rebar fracture load, which was analysed to be due to the insufficient lap length of the rebar. Preliminary tests have shown that the ultimate lap length of restraint grouting-anchoring lap connection of rebar for pre-drilled bellows is  $0.7 l_a$ .

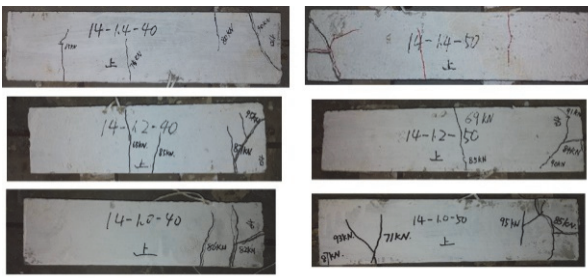


Figure 3 The damage of the specimens with lap rebars of 14 mm

The damage of the specimens with lap rebars of 14 mm is shown in Fig. 3. One or more transverse cracks appeared in the middle of the specimens when loaded near the yielding load.

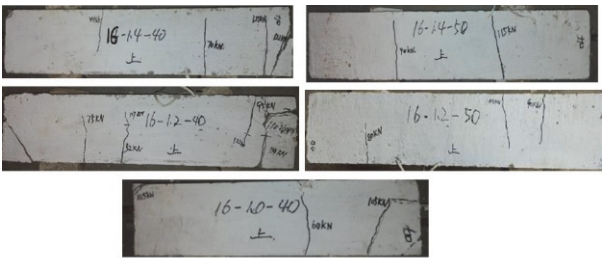


Figure 4 The damage of the specimens with lap rebars of 16 mm

The damage of the specimens with lap rebars of 16 mm is shown in Fig. 4. When the specimen is loaded to the yielding stage, transverse cracks first appear in the middle of the specimen and longitudinal splitting cracks appear at the loading end.

#### 4 ANALYSIS AND DISCUSSION OF EXPERIMENTAL RESULTS

##### 4.1 Analysis of Specimens with Short Lap Lengths of 14 mm and 16 mm Rebar Diameters

To further study and calculate the ultimate lap length, 18 specimens with lap rebars of 14 mm, 16 mm diameter and lap lengths of  $0.6 l_a$ ,  $0.7 l_a$  and  $0.8 l_a$  were concentrated for comparative analysis, which showed that the surface damage of the specimens was more serious than the damage of other specimens with longer lap lengths. Among them, all the specimens with lap length of  $0.7 l_a$  and  $0.8 l_a$  suffered rebar pull-out damage. Five of the 6 specimens with a lap length of  $0.6 l_a$  suffered anchorage damage and one suffered rebar pull-out damage. Below is a specific analysis.

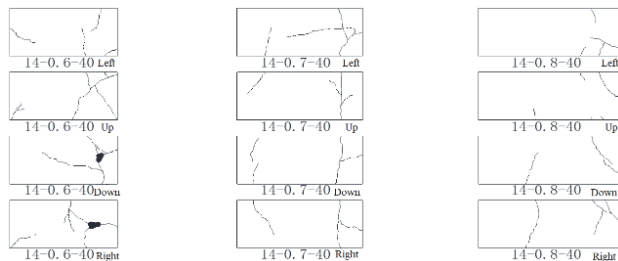


Figure 5 Crack development after loading of specimen 14 -  $l_a$  - 40

Fig. 5 reveals that the cracks in each specimen at different lap lengths of rebar in a 14 mm diameter develop rapidly as the lap length decreases. Although the  $0.7 l_a$  and  $0.8 l_a$  lap length specimens exhibited rebar pull-out damage,

the difference in ultimate load for each specimen was not significant. Overall, the experiment showed that the cracks were mainly concentrated in the transverse cracks at the loading end and no cracks were seen at the anchoring end; the  $0.6 l_a$  specimen exhibited bonded anchorage failure and the ultimate load at failure was significantly less than the two groups of  $0.7 l_a$  and  $0.8 l_a$  specimens. The test showed that the lap length was not sufficient and the specimens showed a cross-linked pattern of longitudinal and transverse cracks at the loading end and longitudinal splitting cracks at the anchoring end while extending towards the middle, with obvious damage to the specimens.

With decreasing lap lengths, the cracking tended to increase in all specimens with different lap lengths of 16 mm rebar diameter. Unlike the 14 mm diameter specimens, the  $0.7 l_a$  and  $0.8 l_a$  lap length specimens showed longitudinal and transverse splitting cracks at the loaded end, and a few longitudinal and transverse cracks at the anchoring end; the shorter  $0.6 l_a$  lap length specimens showed more fully developed cracks, with reticulated cracks all over the specimen surface, indicating a complex internal stress state and significant amplification of the mutual cross-linking (Fig. 6).

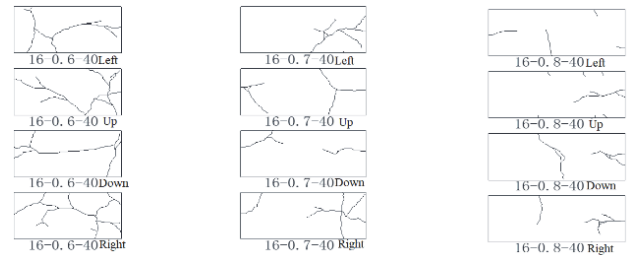


Figure 6 Crack development after loading of 16  $l_a$ , 40 specimen

Transverse cracking cracks were distributed on the specimens, mainly because the internal radial stresses increased continuously when the concrete was subjected to pull-out forces. When the stress value reached the concrete cracking stress  $f_{tk}$ , it caused concrete cracking (Fig. 5 and Fig. 6). The specimen 14 -  $0.7 l_a$  - 40 showed transverse through cracks near the loading end. The surface concrete cracking was serious.

Longitudinal splitting cracks of varying degrees were present in each specimen at the loading end, which were analysed to be due to the circumferential stresses exceeding the concrete cracking strength. The circumferential stresses were caused by the mechanical interaction of the internal rebar and concrete under the action of the taper wedge.

All specimens showed more diagonal corner cracks and dropped corners at the loading end. One reason for this is that the corners are not restricted by the longitudinal concrete and the spiral hoops are relatively widely spaced in this area, reducing the protection. The second is that the matting to balance the eccentric bending moment leads to local stresses, which produce extrusion on the concrete and exacerbate the occurrence of damage. According to the moment balance equation  $F e = P l_a$ , the tensile force  $F$  and eccentric distance  $e$  remain constant, the lap length  $l_a$  decreases inevitably making  $P$  increase, hence the local pressure on the end is greater, leading to the phenomenon of concrete being crushed off. See Fig. 7.

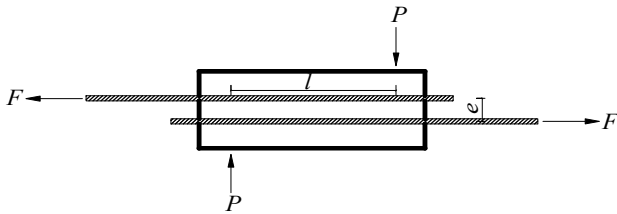


Figure 7 Sketch of eccentric force during loading of the specimen

For 14 mm and 16 mm rebars, 12 specimens with lap lengths of  $0.8 l_a$  and  $0.7 l_a$  were damaged by rebar pulling, while 5 of the 6 specimens with lap lengths of  $0.6 l_a$  suffered severe concrete block damage and the rebar was not broken. We believed that a lap length of  $0.6 l_a$  for reinforcement was not desirable. Considering factors such as structural reliability and actual construction, we suggest that the ultimate connection length of the inserted spiral hoop-bellows be not less than  $0.7 l_a$ . The above tests show that the connection between rebar and grouting material, grouting material and bellows, and bellows and concrete is reliable and can still meet the force requirements with a very short lap length, to ensure that the inserted rebar can fully play a role.

## 5 THEORETICAL ANALYSE

### 5.1 Basic Assumptions of the Theoretical Analysis

In response to the problem studied in this paper and by referring to Xu et al.'s research [21], the basic assumptions of this paper are proposed as follows.

- 1) The use of a converted section for the force section, converting a rectangular to a circular section, which both meets the actual state of force and explains the basis for the adoption of the thick-walled cylinder theory.
- 2) Uniform distribution of bond stresses in the direction of the lap length, irrespective of the effect of the position function.
- 3) The elastic analysis phase, where minor internal displacements can be ignored.
- 4) In the elasto-plastic analysis phase, the concrete stresses are determined and uniformly distributed according to the concrete strains caused by the average slip in the annulus.

Due to the discrete nature of the material itself and the different angles of analysis, a qualitative assessment was given for the correctness of a model only by the theoretical soundness and the error values of the calculated results and the experimental results.

Based on the above four basic assumptions, force models are proposed from the perspective of application. These force models are based on a combination of the degree of damage to the specimen itself and the idea of bounding forces, hoping to provide a quantitative analysis method for the theoretical calculation of the mechanical properties of restraint grouting-anchoring lap connection of rebar.

### 5.2 Boundary Analysis of the Specimen's State of Stress

In the unidirectional pull-out test of restraint grouting-anchoring lap connection of rebar for pre-drilled bellows, two basic damage modes existed in the specimens: rebar pull-out damage and bonded anchor damage, with large

differences in the development of cracks in the specimens. The internal stress variation of the members is more complex. In this paper, with the help of the thick-walled cylinder theory of elastic mechanics, the stress conditions of the concrete and hoop rebar inside each specimen during damage are distinguished, two stress models are derived and the corresponding bearing capacity calculation formulae based on boundary analysis are proposed.

According to the crack development and hoop strain curve, in the sequence from mild to severe damage, the basic stress form of each specimen has two cases: A: when specimen damage happens, the maximum circumferential tensile stress of concrete at the connecting rebar just reaches its standard value of tensile strength  $f_{tk}$ ; B: when specimen damage happens, the crack develops to the hoop, cracking concrete is no longer involved in the work, hoop stress suddenly increases, which should not be negligible. Among them, stress state in case B is often considered by scholars as the limit state of load bearing capacity.

It can be assumed that in this state, the rebar and concrete work together; the rebar strain  $\epsilon_s$  and concrete strain  $\epsilon_c$  are the same; the concrete modulus of deformation  $E'_c$  is used to determine the stress-strain relationship [22]. The stress and strain relationships for concrete and rebar are as follows.

$$\begin{cases} \sigma_c = E'_c \epsilon_c = \gamma E_c \epsilon_c \\ \sigma_s = E_s \epsilon_s \end{cases} \quad (1)$$

where,  $E_c$  is the modulus of elasticity of concrete;  $E_s$  is the modulus of elasticity of rebar;  $\gamma$  is the coefficient of elasticity of concrete.

From Eq. (1) we got:

$$\sigma_s = \frac{E_s}{\gamma E_c} \sigma_c = \frac{\alpha_E}{\gamma} \sigma_c \quad (2)$$

where,  $\alpha_E$  is the ratio of the modulus of elasticity of the rebar to the modulus of elasticity of the concrete.

When the concrete is about to crack at the rebar, there is  $\gamma = 0.5$ , the embedded rebar is spot welded to the hoop rebar, taking the larger hoop stress value of  $\sigma_{sv} = 2\alpha_E \sigma_c$ . The formula for calculating the concrete stress at the hoop rebar is

$$\sigma_c = f_{tk} (D_{cor} - D) / (R - D_{cor}) \quad (3)$$

Take a spiral hoop spacing  $S$  for calculation. From the equilibrium equation of the force we got:

$$(\sigma_{sv} \times 2A_{sv}) / s + \frac{1}{2} f_{tk} (R - D - d) = qd + q_1 D \quad (4)$$

By combining Eq. (1), Eq. (3) and Eq. (4), the ring pressure can be calculated as

$$q = \frac{8\alpha_E A_{sv} f_{tk} (D_{cor} - D) / [(R - D_{cor}) S] + f_{tk} (R - D - d)}{4d} \quad (5)$$

The relationship between the bond stress and the ring pressure provided by the connected rebar can be presented as:

$$\tau = q(\sin \alpha + \mu \cos \alpha) / (\cos \alpha - \mu \sin \alpha) \quad (6)$$

A general formula for the ultimate load carrying capacity can be derived as follows.

$$F_u = \pi \frac{q(\sin \alpha + \mu \cos \alpha)}{\cos \alpha - \mu \sin \alpha} dl_s \quad (7)$$

Combining Eq. (5) and Eq. (7) yields:

$$F_u = \pi \frac{f_{tk} \left\{ \frac{8\alpha_E A_{sv} (D_{cor} - D)}{[(R - D_{cor})S]} + (R - D - d) \right\} (\sin \alpha + \mu \cos \alpha)}{4(\cos \alpha - \mu \sin \alpha)} l_s \quad (8)$$

where,  $\alpha$  is taken as  $30^\circ$  and the friction coefficient  $\mu$  is taken to be 0.4. Substitute the two into the equation and simplify it, then we have

$$F_u = 0.318\pi f_{tk} \left\{ \frac{8\alpha_E A_{sv} (D_{cor} - D)}{[(R - D_{cor})S]} + (R - D - d) \right\} l_s \quad (9)$$

where,  $F_u$  is the ultimate load carrying capacity;  $f_{tk}$  is the standard value of the axial tensile strength of concrete;  $R$  is the cross-sectional dimension of the specimen;  $D$  is the diameter of the bellows;  $d$  is the rebar diameter;  $l_s$  is the lap length;  $\alpha_E$  is the ratio of the modulus of elasticity of the rebar to the modulus of elasticity of the concrete;  $A_{sv}$  is the cross-sectional area of a single spiral hoop;  $D_{cor}$  is the ring diameter of the spiral hoop;  $S$  is the spacing of the spiral hoop.

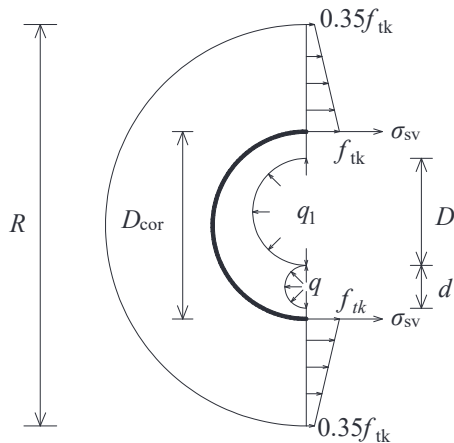


Figure 8 Stress state of concrete section in case-B damage mode

The analysis of the alignment between the calculated results of the damage state in case A and the test results shows that, in the sequence from mild to severe damage, the different states on the type of test piece are summarized as follows.

1) The alignment occurs in specimens with long lap lengths.

2) The overrun condition occurs mostly in specimens with moderate and short lap lengths.

For specimens beyond the damage state in case A, the damage state they meet need to be further analysed. The stress distribution in the concrete section in the case-B damage state is shown in Fig. 8.

According to the above principle of concrete and rebar working together, when the concrete at the hoop is about to crack, the hoop restrains the internal concrete from cracking and quits working; the external concrete at the hoop satisfies  $\gamma = 0.5$  and  $\sigma_c = f_{tk}$ . At this point, the spiral hoop stress is:  $\sigma_{sv} = 2\alpha_E f_{tk}$ ,  $\alpha_E = E_s / E_c$ .

According to the theory of thick-walled cylinders, the proximal stress  $f_{tk}$ , the distal stress is calculated as  $0.35f_{tk}$  (the distal stress value is neglected because it is too small). A spiral hoop spacing  $S$  is taken for calculation and the equilibrium equation of force is obtained as follows.

$$\sigma_{sv} \times 2A_{sv} / S + \frac{1}{2}(f_{tk} + 0.35f_{tk})(R - D_{cor}) = qd + q_1 D \quad (10)$$

Combining Eq. (1) and Eq. (10), the ring pressure can be calculated as:

$$q = \frac{8\alpha_E A_{sv} f_{tk} / S + 1.35 f_{tk} (R - D_{cor})}{4d} \quad (11)$$

Substituting the above equation into Eq. (6) yields

$$F_u = \pi \frac{f_{tk} [8\alpha_E A_{sv} / S + 1.35(R - D_{cor})] (\sin \alpha + \mu \cos \alpha)}{4(\cos \alpha - \mu \sin \alpha)} l_s \quad (12)$$

where,  $\alpha$  is taken as  $30^\circ$  and the friction coefficient  $\mu$  is taken to be 0.4. Substitute the two into the equation and simplify it, then we have

$$F_u = 0.318\pi f_{tk} [8\alpha_E A_{sv} / S + 1.35(R - D_{cor})] l_s \quad (13)$$

Based on the four basic assumptions, two different force models were established and the corresponding bearing capacity calculation equations were derived according to the severity of damage. By comparing the calculated results with the test results, the conclusions are as follows.

1) As the diameter of the rebar increases, the spread of concrete stresses in the specimens becomes more pronounced. The specimens with a rebar diameter of 14 mm have damage states of A and B, while the 16 mm bond-slip damage specimens show damage patterns beyond case B, while the stresses shared by the hoop rebar in the model are increasing, in line with the test findings.

2) The shorter the lap length, the higher the bond stress between the rebar and the concrete interface in the specimen, the damage of the specimen is from mild to severe ( $0.8 l_a$  specimens with damage patterns concentrated in case A,  $0.7 l_a$  and  $0.6 l_a$  specimens with damage patterns concentrated in case B). The test results correspond to the fact that the shorter the lap length, the more pronounced the specimen damage; conversely, the longer the member, the less fully developed the cracks.

3) As the strength of the concrete increases, a larger diameter of rebar and a shorter lap length are required to achieve the same damage pattern in the specimen.

## 6 CONCLUSIONS

The test results show that the connection performance is reliable in the specimen of restraint grouting-anchoring lap connection of rebar for pre-drilled bellows. The test shows that the effective stress transfer between the connected rebar can be ensured at a lap length of  $0.7 l_a$ . The analysis of the crack development shows that the concrete damage tends to become more severe as the lap length decreases; the diameter of the rebar determines the ultimate load carrying capacity of the specimen to a certain extent, and the reduction of the rebar diameter slows down the crack development trend. Based on the four basic assumptions of theoretical analysis, force models are proposed from the perspective of application. These force models are based on a combination of the degree of damage to the specimen itself and the idea of bounding forces, hoping to provide a quantitative analysis method for the theoretical calculation of the mechanical properties of restraint grouting-anchoring lap connection of rebar.

This study demonstrates the reliable performance of restraint grouting-anchoring lap connection of rebar and obtains the key engineering parameters. This will contribute to the promotion of the technology of restraint grouting-anchoring lap connection of rebar, to the promotion of prefabricated buildings, to the advancement of the process of building industrialization, and to the realization of residential industrialization.

## 7 REFERENCES

- [1] Seeber, K., Zong, D. L., Chu, X. F., & Gu, M. W. (2017). Policies and implementation methods related to the development process of prefabricated buildings in the United States. *Residential Industry*, 2017(05), 28-31.
- [2] Song, L. Z., Zhu, J., Liu, S. T., & Qu, Z. J. (2022). Recent Fire Safety Design of High-Rise Buildings. *Journal of Urban Development and Management*, 1(1), 50-57. <https://doi.org/10.56578/judm010106>
- [3] Zou, D. & Sun, C. (2020). Analysis for thermal performance and energy-efficient technology of prefabricated building walls. *Int. J. Heat Technol.*, 38(1), 269-273. <https://doi.org/10.18280/ijht.380129>
- [4] Zou, D. & Sun, C. (2020). Environmental thermal performance of prefabricated buildings based on building wall energy-saving technology. *International Journal of Sustainable Development and Planning*, 15(6), 965-969. <https://doi.org/10.18280/ijstdp.150621>
- [5] Yee, A. A. & Eng, P. H. D. (2001). Social and environmental benefits of precast concrete technology. *PCI Journal*, 46(3), 14-19. <https://doi.org/10.15554/pcij.05012001.14.19>
- [6] Polat, G. (2008). Factors affecting the use of precast concrete systems in the United States. *Journal of Construction Engineering and Management*, 134(3), 169-178. [https://doi.org/10.1061/\(ASCE\)0733-9364\(2008\)134:3\(169\)](https://doi.org/10.1061/(ASCE)0733-9364(2008)134:3(169))
- [7] Polat, G. (2010). Precast concrete systems in developing vs. industrialized countries. *Journal of civil engineering and management*, 16(1), 85-94. <https://doi.org/10.3846/jcem.2010.08>
- [8] Gann, D. M. (1996). Construction as a manufacturing process? Similarities and differences between industrialized housing and car production in Japan. *Construction Management & Economics*, 14(5), 437-450. <https://doi.org/10.1080/014461996373304>
- [9] Noguchi, M. (2003). The effect of the quality-oriented production approach on the delivery of prefabricated homes in Japan. *Journal of Housing and the Built Environment*, 18(4), 353-364. <https://doi.org/10.1023/B:JOHO.0000005759.07212.00>
- [10] Fintel, M. (1995). Performance of buildings with shear walls in earthquakes of the last thirty years. *PCI Journal*, 40(3), 62-80. <https://doi.org/10.15554/pcij.05011995.62.80>
- [11] Ghosh, S. K. (1995). Observations on the Performance of Structures in the Kobe Earthquake of January 17, 1995. *PCI Journal*, 40(2), 14-22. <https://doi.org/10.15554/pcij.03011995.14.22>
- [12] El-Abidi, K. M. A., Ofori, G., Zakaria, S. A. S., & Aziz, A. R. A. (2019). Using prefabricated building to address housing needs in Libya: a study based on local expert perspectives. *Arabian Journal for Science and Engineering*, 44(10), 8289-8304. <https://doi.org/10.1007/s13369-019-03997-2>
- [13] Song, L. Z., Zhu, J., Liu, S. T., & Qu, Z. J. (2022). Recent Fire Safety Design of High-Rise Buildings. *Journal of Urban Development and Management*, 1(1), 50-57. <https://doi.org/10.56578/judm010106>
- [14] Piancastelli, L. (2022). Common Mistakes and Their Fixes in Earthquake-Resistant Buildings. *Acadlore Transactions on Geosciences*, 1(1), 12-21. <https://doi.org/10.56578/atg010103>
- [15] Matic, D., Calzada, J. R., Eric, M., & Babin, M. (2015). Economically feasible energy refurbishment of prefabricated building in Belgrade, Serbia. *Energy and buildings*, 98, 74-81. <https://doi.org/10.1016/j.enbuild.2014.10.041>
- [16] Minunno, R., O'Grady, T., Morrison, G. M., Gruner, R. L., & Colling, M. (2018). Strategies for applying the circular economy to prefabricated buildings. *Buildings*, 8(9), 125. <https://doi.org/10.3390/buildings8090125>
- [17] Navaratnam, S., Ngo, T., Gunawardena, T., & Henderson, D. (2019). Performance review of prefabricated building systems and future research in Australia. *Buildings*, 9(2). <https://doi.org/10.3390/buildings9020038>
- [18] Sagan, V. E., Gergely, P., & White, R. N. (1991). Behavior and design of noncontact lap splices subjected to repeated inelastic tensile loading. *Structural Journal*, 88(4), 420-431. <https://doi.org/10.14359/3037>
- [19] Belleri, A. & Riva, P. (2012). Seismic performance and retrofit of precast concrete grouted sleeve connections. *PCI Journal*, 57(1), 97-109. <https://doi.org/10.15554/pcij.01012012.97.109>
- [20] Kulkarni, S. A., Li, B., & Yip, W. K. (2008). Finite element analysis of precast hybrid-steel concrete connections under cyclic loading. *Journal of constructional steel research*, 64(2), 190-201. <https://doi.org/10.1016/j.jcsr.2007.05.002>
- [21] Xu, Y. L., Wang, H., & Shen, W. D. (1993). Experimental study on the force transmission performance of steel bar lap joint. *Building Structure*, 1993(4), 20-24.
- [22] Shima, H., Chou, L. L., & Okamura, H. (1987). Micro and macro models for bond in reinforced concrete. *Journal of the Faculty of Engineering*, 39(2), 133-194.

**Contact information:**

**Yuzhe SUN**

(Corresponding author)

School of Civil Engineering, Xi'an University of Architecture & Technology, Xi'an  
710055, China

Key Lab of Structural Engineering and Earthquake Resistance, Ministry of  
Education (XAUAT), Xi'an 710055, China

E-mail: sunyuzhe@xauat.edu.cn

**Guoliang BAI**, Professor

School of Civil Engineering, Xi'an University of Architecture & Technology, Xi'an  
710055, China

Key Lab of Structural Engineering and Earthquake Resistance, Ministry of  
Education (XAUAT), Xi'an 710055, China

E-mail: baiglgh@xauat.edu.cn